Characterization of Vitamin A Metabolome in Human Livers With and Without Nonalcoholic Fatty Liver Disease Ⓢ

Guo Zhong, Jay Kirkwood, Kyoung-Jae Won, Natalie Tjota, Hyunyoung Jeong, and Nina Isoherranen

Department of Pharmaceutics, University of Washington, Seattle, Washington (G.Z., J.K., N.T., N.I.) and Department of Pharmacy Practice, University of Illinois, Chicago, Illinois (K.-J.W., H.J.)

Received March 30, 2019; accepted April 25, 2019

ABSTRACT

Retinoids are essential endogenous compounds involved in regulation of critical biologic processes, including maintenance of metabolic homeostasis in the liver. Much of the knowledge of altered retinoid homeostasis in human disease states is derived from changes in indirect markers such as mRNA expression of retinoid-related genes and circulating concentrations of retinol or its binding protein RBP4. We hypothesized that in the human liver, concentrations of the active retinoid all-*trans*-retinoic acid (*at*RA) correlate with the concentrations of retinyl palmitate (RP), the storage form of *at*RA, retinol, the inactive vitamin A, and the mRNA expression of retinoid-related genes. On the basis of existing knowledge of altered vitamin A homeostasis in metabolic syndrome, we also predicted that in human livers with nonalcoholic fatty liver disease (NAFLD) retinoid concentrations would be decreased. Using novel liquid chromatography–tandem mass spectrometry methods, the hepatic vitamin A metabolome was quantified in normal human livers (n = 50) and 22 livers from donors with NAFLD. The hepatic concentrations of RP,

*at*RA, 13-*cis*RA, and 4-oxo-*at*RA were significantly decreased in NAFLD samples in comparison with normal liver samples, whereas retinol levels remained unchanged. The concentrations of *at*RA were positively correlated with RP and 13-*cis*RA but not with retinol or the relative mRNA expression of *LRAT*, *ALDH1A1*, *CYP26A1*, *RARα*, and *RARβ*. An active metabolite of *at*RA, 4-oxo-*at*RA was, for the first time, detected in human tissues at comparable concentration with RA isomers, suggesting this retinoid may contribute to retinoid signaling in humans.

SIGNIFICANCE STATEMENT

This study shows that in NAFLD liver vitamin A homeostasis is disrupted potentially contributing to disease progression. The results show that interpretation of retinoid homeostasis on the basis of indirect markers such as retinol concentrations or mRNA data is probably misleading when evaluating human disease processes, and analysis of the broader retinoid metabolome is needed to characterize disease effects on retinoid signaling.
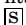
Introduction

Retinoids, which are structural analogs of the inactive vitamin A (retinol, Fig. 1), are essential endogenous compounds involved in regulation of various biologic processes, including adipogenesis and lipid metabolism (Shirakami et al., 2012). Mouse studies have suggested that all-*trans*-retinoic acid (*at*RA) plays a role in enhanced lipid oxidation and reduced fat accumulation in the liver (Kang et al., 2007; Amengual et al., 2010; Kim et al., 2014). On the other hand, it is generally believed that obesity and development of nonalcoholic fatty liver disease (NAFLD) are associated with disturbed vitamin A homeostasis (Shiota, 2005; Graham et al., 2006; Ziouzenkova et al., 2007; Liu et al., 2015; Trasino et al., 2015). In humans, serum retinol concentrations have been

shown to inversely correlate with the progression of NAFLD in a number of studies (Suano de Souza et al., 2008; Villaça Chaves et al., 2008; Botella-Carretero et al., 2010; Chaves et al., 2014; Liu et al., 2015). As such, understanding liver vitamin A homeostasis, its correlation with retinol concentrations, and relationship with NAFLD is important.

The liver plays a key role in regulating vitamin A homeostasis, as retinol is stored via esterification by lecithin retinol acyltransferase (LRAT) as retinyl esters in hepatic stellate cells (O'Byrne and Blaner, 2013). The liver concentrations of the active retinoid all-*trans*-retinoic acid (*at*RA) and the main circulating retinoid, retinol, are believed to be regulated via a complex network of metabolic steps and enzymes (Fig. 1) (Napoli, 2012; Kedishvili, 2016). However, how this network is altered in disease states is not well understood. There is a lack of qualitative and quantitative information about retinoid concentrations and the expression of vitamin A-metabolizing enzymes in human healthy and diseased tissues. In fact, most clinical data related to altered vitamin A homeostasis are derived from indirect measurements of circulating or tissue

ABBREVIATIONS: ACN, acetonitrile; ALDH1A1, aldehyde dehydrogenase 1A1; *at*RA, all-*trans*-retinoic acid; IS, internal standard; LC-MS/MS, liquid chromatography–tandem mass spectrometry; LLOQ, lower limit of quantitation; LOD, limit of detection; LRAT, lecithin retinol acyltransferase; MRM, multiple reaction monitoring; MS/MS/MS, MS3, second generation product ion monitoring; NAFLD, nonalcoholic fatty liver disease; NASH, nonalcoholic steatohepatitis; QC, quality control; RAR, retinoic acid receptor; RP, retinyl palmitate; ROL, retinol.
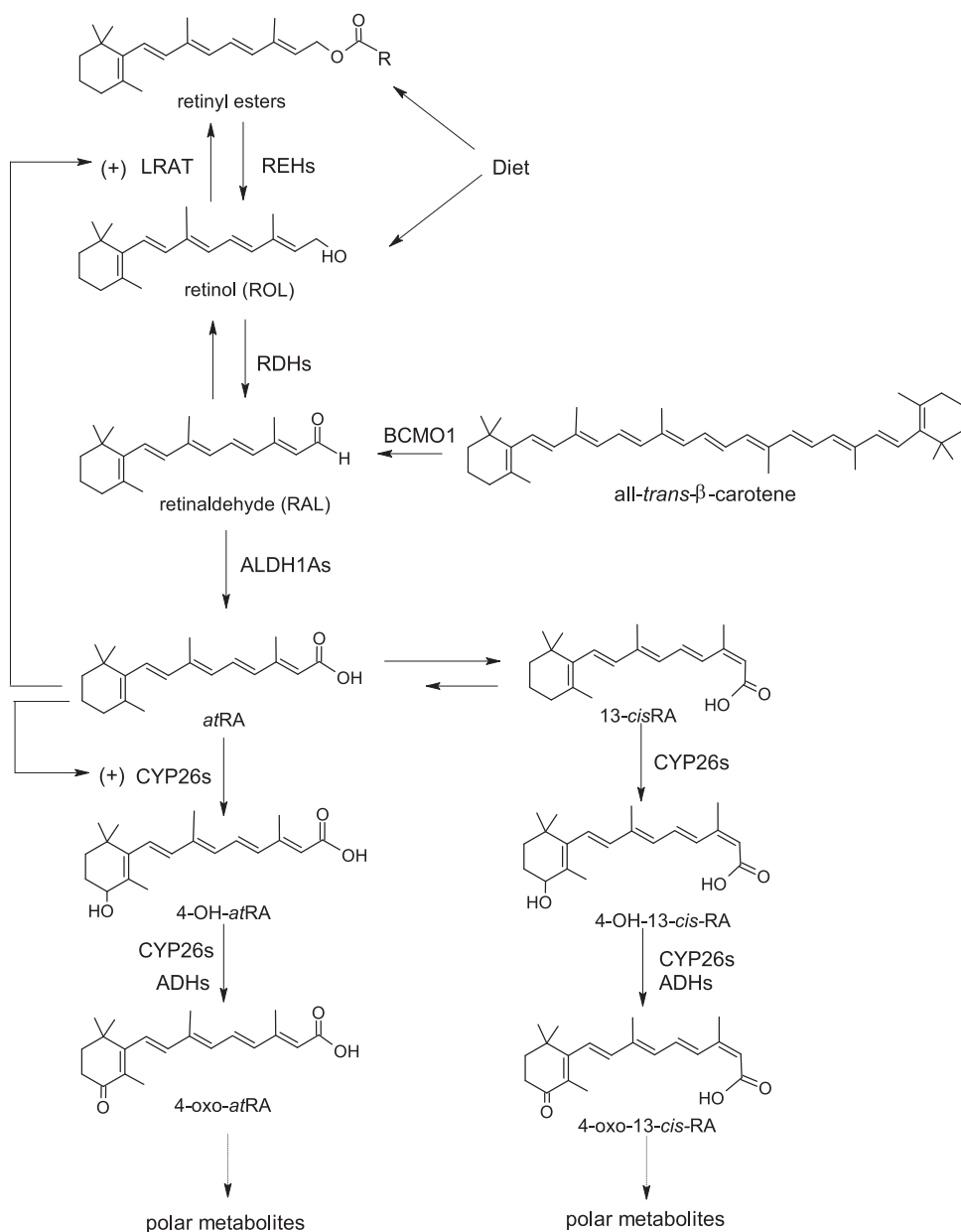
Fig. 1. Metabolic network of retinoid homeostasis shown with chemical structures of retinoids and known metabolic enzymes involved in each step. ADH, alcohol dehydrogenase; BCMO1, β-carotene monooxygenase 1; RDH, retinol dehydrogenase; REH, retinyl ester hydrolase.

retinol concentrations and evaluation of changes in mRNA expression of retinoid-related genes. For example, several studies have shown that circulating retinol and retinol binding protein RBP4 plasma concentrations are significantly altered in diabetes and in NAFLD (Graham et al., 2006; Suano de Souza et al., 2008; Botella-Carretero et al., 2010), but retinoid concentrations, especially *at*RA concentrations, in the liver in these disease states have not been directly measured. In addition, at present no comprehensive characterization of the vitamin A metabolome in human livers has been conducted. As such, the interindividual variability and biologically relevant concentrations in human livers are unknown.

The lack of information on tissue retinoid concentrations and homeostasis is partially a result of the bioanalytical challenges in analyzing retinoids. Retinoids are light-sensitive and have poor mass spectrometric fragmentation. Retinol and retinyl esters have mainly been measured using liquid-liquid extraction and liquid chromatography-UV absorption (LC-UV) (Gundersen and Blomhoff, 2001; Schmidt et al., 2003; Kane and Napoli, 2010). However, retinoids are endogenous compounds and it is impossible to obtain "blank" biologic tissues devoid of retinoids. Therefore, analytical recovery, selectivity, and lack of endogenous interference cannot be easily confirmed. Of special concern is that nearly always the methods have used structurally related but chemically different internal standards, which may not have been adequate to correct for variability in extraction efficiency from different matrices (Schmidt et al., 2003; Obrochta et al., 2014). This is of particular concern when the role of vitamin A homeostasis is assessed in disease states such as NAFLD that involve considerable changes in tissue composition. Fibrosis and fat infiltration for example may alter extraction efficiency and matrix effects and confound the quantification of retinoids. To address these issues, we developed and validated a set of

new liquid chromatography–mass spectrometry (LC-MS/MS) methods to quantify the vitamin A metabolome in human liver using isotope-labeled internal standards and LC-MS/MS–based quantification. Using these quantification methods, our goal in this study was to test the hypothesis that the commonly used indirect markers of atRA concentrations, retinol and retinyl ester concentrations and retinoid-related mRNA expression, correlate with atRA concentrations in human livers from normal and NAFLD donors. We aimed to determine whether measurements of indirect markers or altered atRA concentrations in disease states could be used to define how retinoid signaling networks and metabolism are altered in disease states. Our results show that although NAFLD results in a significantly decreased concentrations of atRA and retinyl esters in human livers, measurement of retinol or retinoid-related mRNA expression fails to accurately capture these changes in retinoid homeostasis. This study shows that to identify the processes that lead to altered vitamin A homeostasis in disease states, the accessible vitamin A metabolome should be characterized.

Materials and Methods

Chemicals and Reagents. atRA and 13-cisRA were purchased from MilliporeSigma (St. Louis, MO). atRA-d$_5$, 13-cisRA-d$_5$, 4-oxo-atRA, 4-oxo-13-cisRA, 4-oxo-atRA-d$_3$, all-trans-retinyl palmitate, and retinol were purchased from Toronto Research Chemicals (North York, ON). All-trans-retinyl palmitate-d$_4$ (RP-d$_4$) and all-trans-retinol-d$_8$ (ROL-d$_8$) were purchased from Cambridge Isotopes (Andover, MA). Blank human serum (DC MASS SPECT GOLD MSG4000) was purchased from Golden West Diagnostics (Temecula, CA). All solvents used in LC-MS/MS analysis were Optima LC-MS grade from Fisher Scientific (Pittsburg, PA).

Liver Samples. To characterize the hepatic vitamin A metabolome in human subjects, 50 de-identified human liver samples were obtained from Corning (Corning, NY). The livers were confirmed by Corning as healthy livers with no major pathology. Relevant donor histories are listed in Supplemental Table S1. This set of samples is referred to as normal samples in this study. The livers were from 39 males and 11 females with donor ages ranging from 21 to 80 years old. Donors included 41 Caucasians, five Asians, three African Americans, and one Hispanic. To investigate if the hepatic vitamin A metabolome is changed in NAFLD, 22 human liver samples were obtained from the Liver Tissue Cell Distribution System (Supplemental Table S2), including nine steatosis (ethnicity unknown; four males and five females) and 13 nonalcoholic steatohepatitis (NASH) samples (10 Caucasians, one Hispanic, two ethnicity unknown; eight males and five females). The diagnosis of steatosis and NASH in these livers was confirmed by histopathology (Supplemental Table S2). The donor ages ranged from 32 to 70 years old. The samples with either steatosis or NASH are together referred to as NAFLD samples in the study. Mouse livers were obtained from C57BL/6X129 mice used in a previous study (Stevison et al., 2017) and all liver samples were from the vehicle control groups in the previous study. All samples were stored in −80°C until analysis.

Sample Preparation. All sample preparation steps for retinoid measurements were performed under yellow light to prevent retinoid isomerization and degradation. As retinyl palmitate is the primary retinyl ester stored in the liver, the hepatic concentration of RP was measured to represent retinyl esters in human liver. To measure RP and retinol, human liver tissue (40–60 mg) was homogenized in a 7:1 ratio of 0.9% saline to tissue weight using Omni Bead Ruptor 24 Bead Mill homogenizer with ceramic beads in methanol-dry ice. The liver homogenate (240 μl) was transferred to a 1.7-ml Eppendorf tube and

spiked with 15 μl of internal standard mixture containing 400 μM RP-d$_4$ and 20 μM ROL-d$_8$. After vortexing, the sample was left on ice for 10 minutes, followed by addition of 1 ml ice-cold acetonitrile (ACN) to precipitate protein. The sample was vortexed and placed on ice for 20 minutes before centrifugation. After the sample was centrifuged at 18,000g at 4°C for 30 minutes to pellet liver protein, the supernatant was collected. A 50-μl aliquot of the supernatant was diluted with 950 μl of 80% ACN for the LC-MS/MS analysis of RP. The rest of the supernatant was transferred to amber LC-MS vials for the LC-MS/MS analysis of retinol.

To measure atRA, 13-cisRA, and 4-oxo-atRA in human liver, a liquid-liquid extraction was adapted and modified from a published method (Obrochta et al., 2014). Liver tissues (80–100 mg) were homogenized in a 2-ml Potter-Elvehjem glass homogenizer (Kimbel Glass, Vineland, NJ) on ice with a ratio of 5:1 of 0.9% saline to tissue weight. The Bead Mill homogenizer was not used for liquid-liquid extraction because the ceramic beads used for homogenization caused technical difficulties for the performance of liquid-liquid extraction. The homogenate was transferred with a Pasteur pipette to a 15-ml glass culture-tube on ice and was spiked with 10 μl of internal standard (IS) mixture containing 500 nM atRA-d$_5$, 13-cisRA-d$_5$, and 4-oxo-atRA-d$_3$. To this mixture, 2 ml of 25 mM KOH in ethanol was added, and the sample was vortexed. Ten milliliters of hexanes were then added, and the sample was vortexed and centrifuged at 300g for 2 minutes to separate organic phase from aqueous phase. The top hexane layer was removed using a Pasteur pipette, and 120 μl of 4 M HCl was added to the aqueous layer of the sample. The sample was quickly vortexed, followed by the addition of 10 ml of hexanes to extract atRA and 13-cisRA. After centrifugation at 300g for 2 minutes, the top hexane layer containing RA isomers was removed using a Pasteur pipette to a new glass culture tube on ice. Ethyl acetate (10 ml) was then added to the aqueous sample phase followed by 2 ml of water to enhance phase separation to extract 4-oxo-atRA. After centrifugation at 300g for 15 minutes, the top ethyl acetate layer containing 4-oxo-atRA was transferred to a new glass culture tube on ice using a Pasteur pipette. The organic layers were dried down at 35°C under a gentle N$_2$ flow and then placed on ice. Residues containing RA isomers (from hexane extraction) or 4-oxo-atRA (ethyl acetate extraction) were resuspended into 60 μl of ACN and transferred to amber mass spectrometry vials with glass inserts using Pasteur pipettes. Right before the LC-MS/MS analysis, water (40 μl) was added to the ACN resuspensions to improve chromatographic resolution.

LC-MS/MS Analysis. Three LC-MS/MS methods for the analysis of RP, retinol, RA isomers, and 4-oxo-RA isomers were developed. All LC-MS/MS analyses were performed under positive ion mode using atmospheric pressure chemical ionization and nitrogen as the collision and curtain gases. The analytical column (2.1 × 150 mm, 2.7 μm) and guard column (2.1 × 5 mm, 2.7 μm) used for analyte separation were both Ascentis Express RP-amide columns from MilliporeSigma. The autosampler was set at 6°C. To measure RA isomers and 4-oxo-atRA, the LC-MS/MS analysis was performed on an AB Sciex 5500 QTRAP Mass Spectrometer (AB Sciex LLC, Framingham, MA) coupled with an Agilent 1290 UHPLC (Agilent Technologies, Santa Clara, CA). RP and retinol were measured using AB Sciex 6500 QTRAP Mass Spectrometer coupled with Shimadzu UFLC XR DGU-20A5 (Shimadzu Corporation, Kyoto, Japan). For all the LC-MS/MS analyses, mobile phases A and B were water with 0.1% formic acid (FA) and ACN with 0.1% FA, respectively. To measure retinol and RP, the injection volume, LC flow rate, and column temperature were set at 4 μl, 0.4 ml/min, and 40°C. The LC condition started at 60% B for 2 minutes, followed by a gradient to 66% B by 9.2 minutes, and then to 100% B by 13 minutes, and then kept at 100% B for 10 minutes before the return to starting conditions. To measure RA isomers, the injection volume, LC flow rate, and column temperature were set at 20 μl, 0.4 ml/min, and 25°C. The LC condition started at 70% B for 3 minutes, then increased linearly to 78% B by 12 minutes, then changed to 100% B, and was kept at that for 3 minutes before return to starting condition. For 4-oxo-RA

TABLE 1

MS parameters used in LC-MS/MS and LC-MS/MS/MS analysis

Analyte	MRM (MS^3)	DP (V)	EP (V)	CE (V)	GS1	GS2
ROL and RP	m/z 269 > 93, 95	35	4	30	70	70
ROL-d$_8$	m/z 277 > 98, 102	35	4	30	70	70
RP-d$_4$	m/z 273 > 94, 98	35	4	30	70	70
*at*RA and 13-*cis*RA	m/z 301 > 205 (m/z 301 > 205 > 159)	60	10	17	80	0
*at*RA-d$_5$ and 13-*cis*RA-d$_5$	m/z 306 > 208 (m/z 306 > 208 > 162)	80	10	17	80	0
4-oxo-*at*RA and 4-oxo-13*cis*RA	m/z 315 > 137, 147, 241	50	10	29, 26, 20	60	70
4-oxo-*at*RA-d$_3$	m/z 318 > 137	50	10	29	60	70

CE, collision energy; DP, declustering potential; EP, entrance potential; GS, gas.

measurements, the injection volume, LC flow rate, and column temperature were set at 20 μl, 0.5 ml/min, and 40°C. The LC conditions started at 40% B for 2 minutes, followed by a gradient to 67% B by 9 minutes, then changed to 100% B, and maintained for 2 minutes before the return to the starting conditions. All retinoids were analyzed and the concentrations quantified on the basis of multiple reaction monitoring (MRM), whereas MS/MS/MS (MS^3, second generation product ion monitoring) data were collected in parallel for measurement of RA isomers and for confirmation of analyte identity (Table 1). MS parameters used in all three LC-MS/MS methods were: temperature 350°C, nebulizer current 5 μA, curtain gas 35 psi, collision-associated dissociation −2 psi and cell exit potential 10 V. All other MS parameters are listed in Table 1. In MS^3 mode, which was set up to monitor RA isomers, product ions [M+H]$^+$ derived from the precursor ion of the MRM transition were collected, ranging from m/z 109 to 220 Da. The Q$_1$ resolution was set to low and the Q$_0$ trapping was turned on. The Q$_3$ entry barrier was 8 V and the scan rate 10,000 Da/s. The linear ion trap (LIT) fill time was 250 milliseconds, except for the internal standards, for which the fill time was 50 milliseconds.

Enhanced product ion (EPI) scans were collected to confirm the identity of 4-oxo-RA isomers in human liver. The MS/MS spectra of the [M+H]$^+$ ion, m/z 315.2 Da, were collected within the mass range of m/z 50–340 Da. EPI scan rate was set at 10,000 Da/s, LIT fill time at 100 milliseconds, Q$_1$ at low resolution, and Q$_3$ entry barrier at 8 V. The Q$_0$ trap was turned on. The LC conditions and other MS parameters were the same as those described above for the measurement of 4-oxo-RA isomers.

Method Validation. The methods used for retinoid concentration measurements were validated following the FDA guidance on bioanalytical method validation (FDA, 2018), adapted for endogenous compounds. Owing to the lack of blank retinoid-free liver tissue, charcoal-treated blank human serum free of retinoids was used as a blank matrix. For method development, the blank human serum was diluted with 5× volume of 0.9% saline, and used to prepare standard-curve samples and three quality control samples (QC 1–3) spiked with the retinoids in low, low-medium, or medium-high concentration. The range of standard curves and QC concentrations for all the analyzed retinoids are listed in Table 2. As a further validation to assess extraction variability in the liver tissue matrix, human liver samples from six donors were homogenized with 5:1 0.9% saline/tissue weight, the homogenates pooled, and stored as aliquots at −80°C for analysis as liver QC samples (LQCs). During validation, diluted serum or 540 μl of pooled liver homogenate per analysis were used to measure RA isomers and 4-oxo-*at*RA, and 240 μl per analysis were used for retinol and RP measurements. All samples were processed and analyzed with corresponding LC-MS/MS methods as described above. The peak areas of analyte and IS were integrated using Analyst software version 1.6.3 (AB Sciex LLC). To build standard curves, the peak area ratio of analyte to IS was plotted as a function of serum retinoid concentration. All QCs and LQCs were prepared in six replicates per day and validation assays were repeated on three separate days to determine intraday and interday coefficient of variation (%CV). Retinoid standards, including RA and 4-oxo-RA dissolved in 60% acetonitrile, and retinol and RP dissolved in 80% acetonitrile, were

TABLE 2

Method validation data for the analyzed retinoids

The measured concentrations are the mean concentrations of interday measurements.

| Analyte		*at*RA	13-*cis*RA	4-oxo-*at*RA	Retinol	RP
Standard curve concentration range (in serum)		1–1000 nM	1–1000 nM	2.7–444 nM	0.15–37.5 μM	3–750 μM
Linearity (R^2)		0.998	0.999	0.999	0.999	0.993
QC1	Known concentration	1.6 nM	1.6 nM	7.6 nM	0.4 μM	7.8 μM
	Measured concentration	1.6 nM	1.6 nM	7.5 nM	0.4 μM	7.6 μM
	Accuracy%	100.1	96.6	98.8	98.0	97.8
	Intraday CV%	8.9	8.7	4.7	7.3	7.1
	Interday CV%	8.8	8.4	4.9	8.4	11.3
QC2	Known concentration	25.9 nM	25.9 nM	47.4 nM	1.6 μM	31.3 μM
	Measured concentration	24.9 nM	25.1 nM	45.7 nM	1.5 μM	30.9 μM
	Accuracy%	96.1	96.8	96.5	96.5	98.9
	Intraday CV%	3.2	3.6	3.5	5.3	6.6
	Interday CV%	3.3	5.6	3.7	6.7	8.5
QC3	Known concentration	222 nM	222 nM	296 nM	6.3 μM	125 μM
	Measured concentration	202 nM	216 nM	291 nM	6.0 μM	121 μM
	Accuracy%	91.1	97.2	98.1	96.5	96.6
	Intraday CV%	3.8	6.1	2.9	5.0	7.1
	Interday CV%	7.4	6.7	3.2	8.0	6.9
Liver QC	Measured concentration	139.5 pmol/g	31.3 pmol/g	188.5 pmol/g	2.2 nmol/g	66.2 nmol/g
	Intraday CV%	5.3	6.2	5.2	6	12.3
	Interday CV%	8.8	11.9	8.9	10.1	15.2

CV, coefficient of variation.

used to determine on-column limit of detection (LOD; signal-to-noise >3 to 1) and lower limit of quantitation (LLOQ; signal-to-noise >5 to 1). Owing to the lack of "blank" liver tissue, LOD and LLOQ in matrix were not measured. To confirm the validity of the approach of using blank serum as a reference matrix instead of liver to construct standard curves, mouse liver homogenates (540 μl per analysis for RA and 4-oxo-RA isomers and 240 μl per analysis for retinol and RP) were also spiked with retinoids to build standard curves and samples were processed and analyzed as described above in parallel with serum standard curves. The slopes of standard curves for each retinoid were compared between the two matrices to test for a systematic matrix effect and to verify similar concentration-response in the two matrices.

mRNA Expression in Human Liver Samples. Total RNA was extracted from human liver tissues using TRIzol reagent (Invitrogen, Carlsbad, CA), and was reverse-transcribed into cDNA using High-Capacity cDNA Reverse Transcription Kit (Life Technologies, CA). Real-time PCR was performed using StepOnePlus Real-Time PCR System with PrimeTime probes (Integrated DNA Technologies, Coraville, IA). The mRNA expression of aldehyde dehydrogenase 1A1 (*ALDH1A1*), *LRAT*, *CYP26A1*, retinoic acid receptor (*RAR*)α, and *RARβ* was measured in 48 out of the 50 normal human livers. *GAPDH* was used as the housekeeping gene. The mRNA expression of *ALDH1A1*, *LRAT*, *CYP26A1*, *RARβ*, and *RBP4* was also measured in 22 NAFLD samples and in parallel in nine randomly selected normal liver samples with *GAPDH* as the housekeeping gene. The following primers purchased from Integrated DNA Technologies were used: *ALDH1A1* (Hs.PT.56a.38450309), *CYP26A1* (Hs.PT.58.2905296), *LRAT* (Hs.PT.58.39384980), *RARα* (Hs.PT.58.2437218), *RARβ* (Hs.PT.58.364456), *RBP4* (Hs.PT.58.38653618), and *GAPDH* (Hs.39a.22214836). The relative mRNA expression level normalized to the housekeeping gene was calculated using the $2^{-\Delta\Delta Ct}$ method and comparing the expression in individual donors to the mean of all livers (Livak and Schmittgen, 2001).

Data Analysis. For both normal and NAFLD liver samples, retinoid concentrations in liver and the mRNA expression of retinoid homeostasis-related genes were first log-transformed and Grubb's test was used to test for the presence of outliers in each retinoid group and each gene group. Spearman's rank-order correlation was done to analyze correlations of the hepatic *at*RA concentration with other retinoid concentrations and the mRNA expression of retinoid homeostasis-related genes in normal livers. Because multiple comparisons were done in the correlation analyses, a Bonferroni
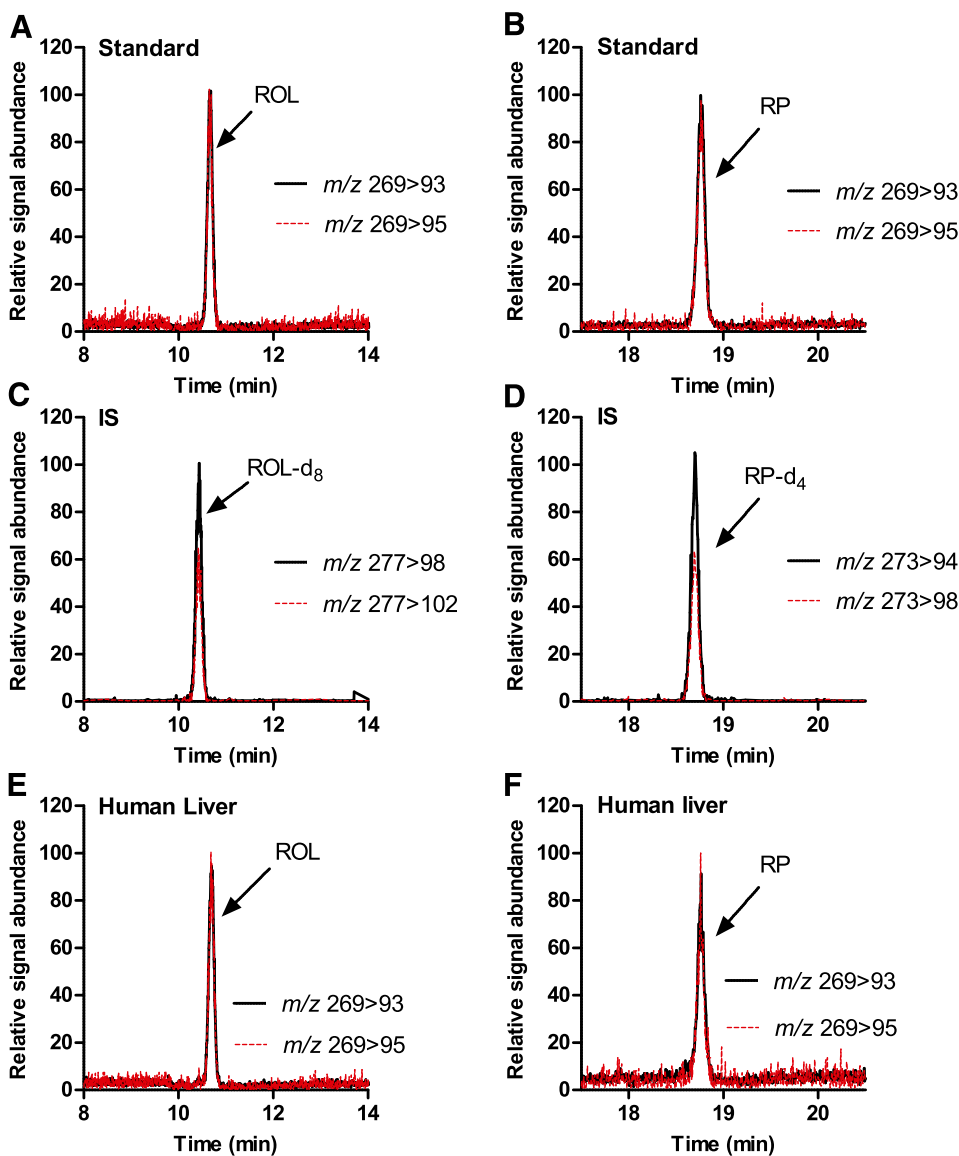
Fig. 2. Detection of retinol and retinyl palmitate in human liver. (A–D) MRM chromatograms of synthetic standards and internal standards spiked into blank serum and processed as described in *Materials and Methods*. (E and F) MRM chromatograms of ROL and RP in a pooled human liver homogenate ($n = 6$).

adjustment was used to adjust *P* value (0.05/9) and a *P* value less than 0.005 was considered significant. To compare NAFLD livers with normal liver samples, significant differences in retinoid concentrations and the relative mRNA expression of retinoid-related genes among the normal, steatosis, and NASH group were analyzed by Kruskal-Wallis test followed by Dunn's multiple comparison test. The Spearman's rank-order correlation was used to analyze correlations of *at*RA concentrations with other retinoid concentrations in all measured human liver samples. A *P* value less than 0.01 (Bonferroni adjusted *P* value 0.05/4) was considered significant. Spearman's rank-order correlation was also used in an exploratory analysis to test for correlation between donor age and retinoid concentrations. Differences in retinoid concentrations between male and female donors were tested using two-tailed students *t* test.

Results

Detection of Vitamin A Metabolome in Human Livers. All measured retinoids in human liver were separated and detected using the corresponding LC-MS/MS methods. The developed methods allowed specific and sensitive LC-MS/MS-based detection and quantification of retinol, RP, *at*RA, and 13-*cis*RA in human livers (Figs. 2 and 3). In addition, for the first time, 4-oxo-*at*RA and 4-oxo-13-*cis*RA were detected in the human liver (Fig. 4). The retention times of all analytes detected in human liver matched with those of synthetic standards and isotope-labeled internal standards. The retention times and relative signal intensities of *at*RA and 13-*cis*RA peaks identified on the basis of the MRM scans corresponded to those observed in MS[3] scans, indicating correct identification and lack of interference in the peaks and mass transitions selected to quantify *at*RA and 13-*cis*RA (Fig. 3). In addition, peaks with retention times around 7.9 and 9.1 minutes were detected in the human liver MRM chromatograms in the same

transition as RA (Fig. 3), which appear to be nonretinoid-related interfering peaks on the basis of the considerably lower signal intensity in the RA-specific MS[3] transition compared with *at*RA and 13-*cis*RA (Fig. 3). This finding is similar to what has been reported previously for mouse tissues and human testis (Kane et al., 2008; Arnold et al., 2015).

To confirm the identity of 4-oxo-*at*RA and 4-oxo-13-*cis*RA in human liver, MS/MS spectra were collected for the tentative peaks and compared with the spectrum collected for the reference standard (Fig. 4). The collected spectra showed a fragmentation pattern of the tentative 4-oxo-*at*RA in human liver that matched with the spectrum of 4-oxo-*at*RA synthetic standard, confirming that the identified peak was indeed 4-oxo-*at*RA. 4-oxo-13-*cis*RA was also detected in human liver and an MS/MS spectrum was collected for this analyte as well. Owing to the low signal intensity of 4-oxo-13-*cis*RA in human liver (Fig. 4), high background noise was detected in the spectrum of the peak eluting at the same retention time as 4-oxo-13-*cis*RA standard, making the identification of this peak equivocal. However, product ions of *m/z* 137, 147, 159, and 241 were detectable, suggesting that the peak is 4-oxo-13-*cis*RA (Fig. 4). In mouse liver, 4-oxo-*at*RA was detected but its concentration was below LLOQ, and 4-oxo-13-*cis*RA was not detected (Fig. 4).

Method Validation. On the basis of preliminary experiments, the concentrations of RP and retinol were >1000-fold higher than those of RA isomers and 4-oxo-*at*RA within the human liver. RP was present in pooled liver homogenates (*n* = 6) at a concentration of 66 nmol/g of liver and retinol was about 2 nmol/g of liver, and the concentrations of *at*RA and 13-*cis*RA were about 140 and 39 pmol/g of liver, respectively. Hence, it is impossible to quantify the vitamin A metabolome in a single analytical LC-MS/MS run owing to the dynamic
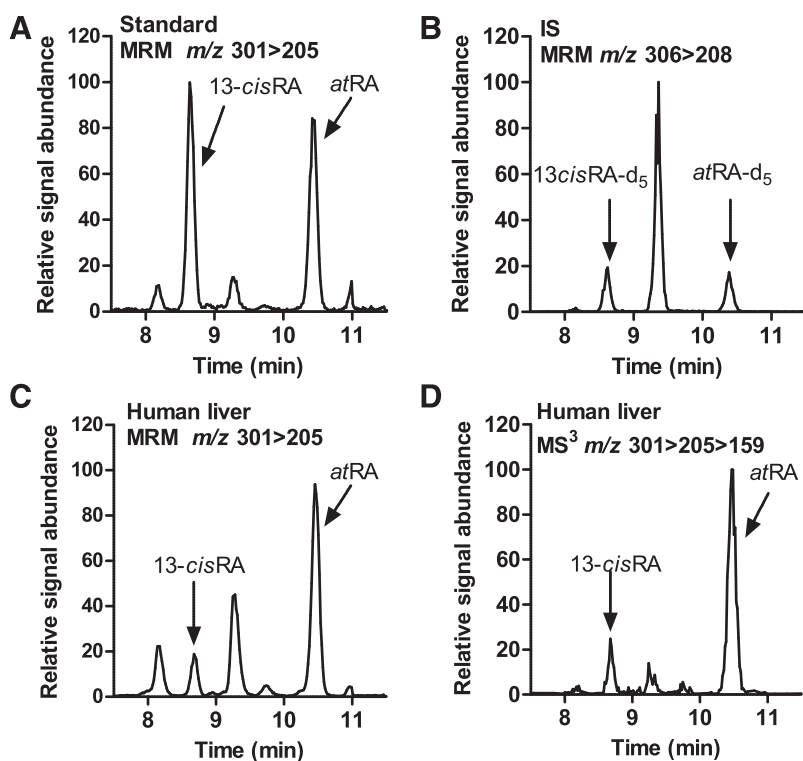
Fig. 3. Detection of *at*RA and 13-*cis*RA in human liver. (A and B) MRM chromatograms of synthetic standards and internal standards spiked into blank serum and extracted as described in *Materials and Methods*. (C) MRM chromatogram of *at*RA and 13-*cis*-RA in a pooled human liver homogenate (*n* = 6). (D) Selected ion–extracted LC-MS/MS/MS (MS[3]) chromatogram (*m/z* 301 > 205 > 159) of *at*RA and 13-*cis*RA in the same liver sample depicted in (C).
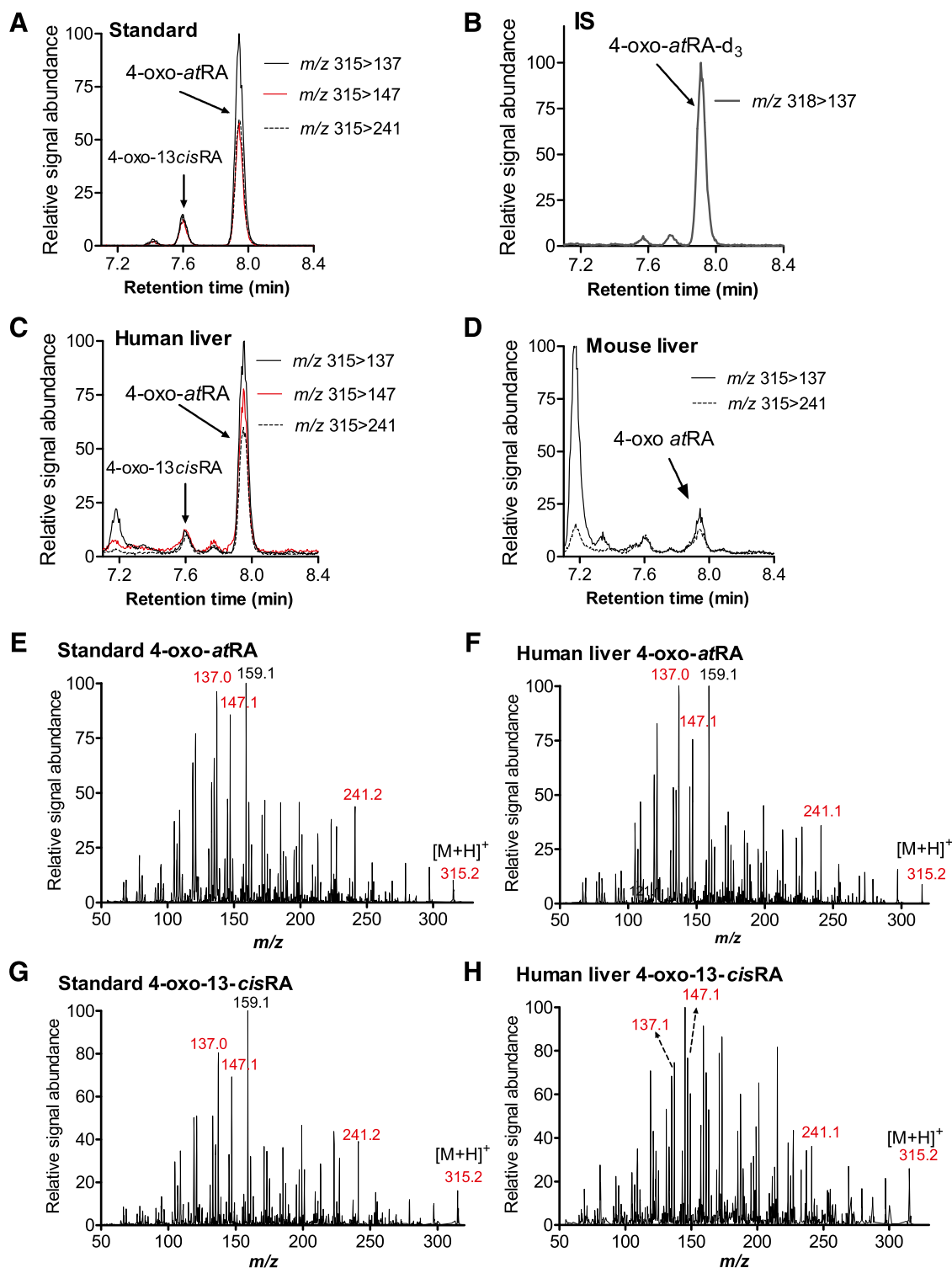
Fig. 4. Detection and identification of 4-oxo-*at*RA and 4-oxo-13-*cis*RA in human liver. (A–D) Representative MRM chromatograms of 4-oxo-*at*RA, 4-oxo-13-*cis*RA, and 4-oxo-*at*RA-d$_3$ as detected from reference standards (A and B), from a pooled human liver homogenate ($n = 6$) (C), and from mouse liver shown for comparison (D). In mouse liver the concentration of 4-oxo-*at*RA was below LLOQ and 4-oxo-13-*cis*RA was not detected. (E–H) MS/MS spectra of 4-oxo-*at*RA and 4-oxo-13-*cis*RA with (E) and (G) being from reference standards dissolved in 60% ACN, and (F) and (H) of the peaks detected from pooled human liver and identified as 4-oxo-*at*RA and 4-oxo-13-*cis*RA. The parent ion (m/z 315.2) and product ions selected for MRM are indicated in red color. In (A), (B), (E), and (G) 4-oxo-*at*RA, 4-oxo-13-*cis*RA, and 4-oxo-*at*RA-d$_3$ concentrations are 500, 100, and 100 nM, respectively. In (C) 4-oxo-*at*RA concentration was measured as 188.5 pmol/g liver.

range limitations of modern LC-MS/MS instruments. In this study, the high-concentration retinoids (retinol and RP) were analyzed separately after protein precipitation

with acetonitrile, and the acidic metabolites (RA isomers and 4-oxo-*at*RA) were analyzed in two separate methods owing to the requirement of different organic extraction
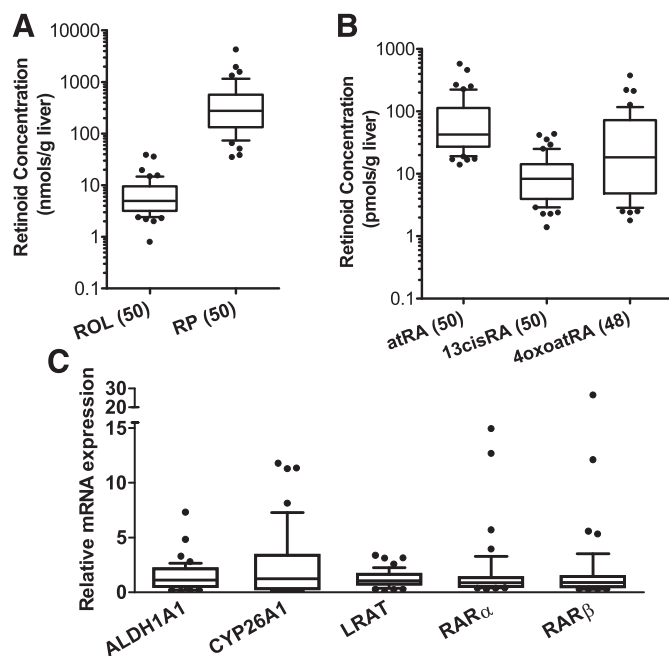
Fig. 5. Hepatic retinoid concentrations (A and B) and relative mRNA expression of retinoid-related genes (C) in normal human liver samples. The box, horizontal line, and whiskers represent interquartile range (IQR), median, and 10%–90% percentile, respectively. (A) Hepatic concentrations of RP and ROL and (B) those of *at*RA, 13-*cis*RA, and 4-oxo-*at*RA. Numbers in brackets on the *x*-axis indicate the number of livers included in the plots for each retinoid. *Y*-axis is shown in log scale. In (C) the relative mRNA expression was analyzed in 48 normal human liver samples and was calculated using $2^{-\Delta\Delta Ct}$ method with *GAPDH* as the house-keeping gene as described in the materials and methods.

solvents for analyte recovery. 4-oxo-RA isomers could not be detected in tissue samples and serum using hexane extraction because of poor recovery. Likewise, extraction of RA from tissues using ethyl acetate resulted in poor chromatographic quality and a high level of interference from liver samples (data not shown). Therefore, a two-step extraction method was adapted for RA and 4-oxo-RA isomers.

The methods for quantification of vitamin A and its metabolites were validated using isotope-labeled retinoids as internal standards. On-column LOD and LLOQ of measured retinoids (in the absence of matrix) were 13 and 27 fmol for *at*RA, 19 and 38 fmol for 13-*cis*RA, 26 and 49 fmol for 4-oxo-*at*RA, 15 and 30 fmol for retinol, and 30 and 60 fmol for RP, respectively. The slopes of standard curves constructed using serum and liver were similar for the measurement of RP, retinol, *at*RA, 13-*cis*RA, and 4-oxo-*at*RA

(Supplemental Fig. S1), demonstrating that the deuterium-labeled internal standards appropriately correct for matrix effects from the liver. The *y*-axis intercept was generally higher for the liver standard curves than serum, indicating the detection of the endogenous retinoids in the liver matrix (Supplemental Fig. S1). However, for 4-oxo-13-*cis*RA, the slopes of the standard curves were different between the two matrices, demonstrating the confounding effect of using nonidentical chemical internal standards (4-oxo-*at*RA-d₃) for normalization. It is probable that the chromatographic separation of 13-*cis*- and all-*trans*-isomers results in different matrix effects for the two isomers, confounding the quantification of 4-oxo-13-*cis*RA when 4-oxo-*at*RA-d₃ is used as the internal standard. Thus, in the current study, 4-oxo-13-*cis*RA was not quantified even though the analyte was detectable in all liver samples.

The method validation results are shown in Table 2. Considering the biologic variability of retinoid concentrations in human tissues, the ranges of standard curves were designed to be wide enough to cover retinoid concentrations in all measured liver samples. All standard curves were linear within the ranges analyzed, with R^2 values higher than 0.99. The percentage of error of all QCs was less than 15% compared with true values. Interday and intraday CV% of all QCs and LQCs including the pooled liver sample showed that variability within day and between days was less than 15%, confirming the reproducibility of the method.

The Vitamin A Metabolome in Normal Human Livers. Hepatic concentrations of each measured retinoid in 50 normal liver samples showed log-normal distribution, with high variability but with no identified outliers in the dataset (Fig. 5). Retinol ($n = 50$), RP ($n = 50$), *at*RA ($n = 50$), 13-*cis*RA ($n = 50$), and 4-oxo-*at*RA ($n = 48$) were all detected in the liver samples analyzed. Hepatic concentrations of retinol and RP were in the range of nmol/g of liver, much higher than other measured retinoids, which were in the range of picomoles per gram of liver. On the basis of the median concentrations (Fig. 5; Table 3), hepatic RP concentration was about 19-fold higher than retinol. Compared with *at*RA concentrations in the liver, 13-*cis*RA had lower median concentration with less interindividual variability. The hepatic 4-oxo-*at*RA concentration was consistently lower than *at*RA (45 of 48 livers) with only two liver samples having higher 4-oxo-*at*RA concentrations than *at*RA and one sample having similar *at*RA and 4-oxo-*at*RA concentrations. The *at*RA concentration in normal human livers was positively correlated with the concentration of RP, retinol, 13-*cis*RA,

TABLE 3
Hepatic concentrations of retinoids in normal and NAFLD liver samples

	Normal (n = 50)		Steatosis (n = 9)		NASH (n = 13)	
	Median	Range	Median	Range	Median	Range
RP (nmol/g)	276	12.6–4282	59.7	1.3–285.1	71.9[a]	3.4–153.3[a]
Retinol (nmol/g)	14.1	1.2–161	8.1	0.8–13.4	32.5	0.2–47.2
*at*RA (pmol/g)	42.6	14.0–579.5	29.8	18.3–34.7	23.3	9.3–35.2
13-*cis*RA (pmol/g)	8.3	1.4–43.5	5.1	3.1–6.2	5.3	2.7–7.9
4-oxo-*at*RA (pmol/g)	18.3[b]	1.8–376.3[b]	2.5	1.8–7.6	5.9	0.9–22.1

[a]The RP concentration in one NASH sample was below LOD. Hence, the RP concentration in that sample was excluded and 12 liver samples were included in the analysis of RP concentrations for the NASH group.
[b]4-Oxo-*at*RA concentrations were measured in 48 samples in the normal group.

TABLE 4

Spearman correlation of *at*RA concentration with other retinoid concentrations and the mRNA expression of retinoid-related genes in human livers

The group of normal livers includes n = 50 livers free of known NAFLD pathologies. The normal and NAFLD group includes all the livers in the normal group and the additional livers with pathologically characterized fatty liver and cirrhosis (Supplemental Tables S1 and S2).

|	Normal only (*n* = 50)		Normal and NAFLD (*n* = 72)	
*at*RA vs.	Spearman *r*	*P* value	Spearman *r*	*P* value
RP	0.48	0.0004[a]	0.48	<0.0001[b]
Retinol	0.43	0.0016[a]	0.29	0.015
13-*cis*RA	0.83	<0.0001[a]	0.82	<0.0001[b]
4-oxo-*at*RA	0.82	<0.0001[a]	0.71	<0.0001[b]
LRAT	0.26	0.067		
ALDH1A1	−0.29	0.046		
CYP26A1	0.14	0.33		
RARα	−0.14	0.34		
RARβ	0.02	0.92		

[a]$P < 0.005$; a Bonferroni adjusted *P* value of 0.005 (0.05/9) was used to indicate significance for normal liver samples.
[b]$P < 0.01$; a Bonferroni adjusted *P* value of 0.01 (0.05/4) was used to test for significance of correlation for normal and NAFLD samples.

and 4-oxo-*at*RA, with *P* values <0.005 (Table 4). The correlation between hepatic concentration of retinol and RP was also analyzed using Spearman rank correlation, and showed an *r* of 0.36 ($P = 0.011$). In an exploratory analysis of sex differences in retinoid metabolome no differences were observed between male and female donors for any of the retinoids (data not shown). Likewise, no correlation was observed between donor age and retinoid concentrations in the liver. This lack of correlation and sex differences may be owing to the retrospective nature of the analysis and lack of ability to adjust for covariates in the analysis.

Vitamin A Homeostasis Is Disrupted in Liver Samples with NAFLD Compared with Normal Liver Samples. Intended retinoids were detected in all NAFLD samples (nine steatosis and 13 NASH) except one NASH liver sample in which RP concentration was below LOD (in three repeated, independent analyses). The RP concentration in this liver was excluded from the data shown in Fig. 6A. Hepatic *at*RA, 13-*cis*RA, and RP concentrations were significantly lower in NASH liver samples than in normal liver samples and there was a trend toward lower concentrations in steatosis samples, but this difference did not reach statistical significance (Fig. 6; Table 3). In addition, compared with liver samples in the normal group, both steatosis and NASH samples had significantly lower concentrations of 4-oxo-*at*RA (Fig. 6). Together these data demonstrate significant retinoid depletion in NASH and indicate a progressive depletion of retinoids with NAFLD severity. No significant differences in hepatic ROL concentrations were observed between the normal and steatosis livers or between the normal and NASH group, indicating that ROL concentrations are maintained in the liver despite depletion of other retinoids (Fig. 6B; Table 3). The positive correlation between hepatic *at*RA and other retinoid concentrations (RP, 13-*cis*-RA, and 4-oxo-*at*RA) observed in normal livers remained unchanged when NAFLD samples were included. However, the correlation between *at*RA and retinol was no longer significant when NAFLD samples were included (Table 4), suggesting that independent measurements of the different retinoids are needed to assess retinoid status in disease states.
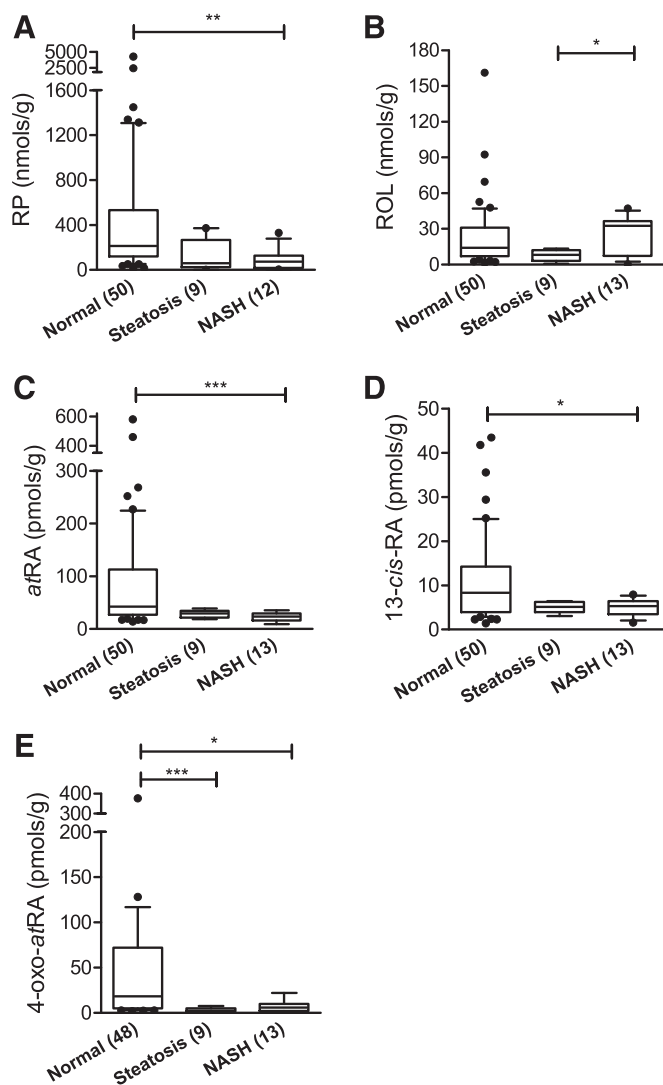
Fig. 6. Box and whiskers plots of retinoid concentrations in a subset of normal human livers and NAFLD human liver samples. (A) Retinyl Palmitate, (B) Retinol, (C) all-trans-Retinoic acid, (D) 13-cis-retinoic acid, (E) 4-oxo-all-trans-Retinoic acid. The liver disease stage is shown in the *x*-axis. Significant differences between the three groups were tested with Kruskal-Wallis test followed by Dunn's multiple comparison test; *$P < 0.05$; **$P < 0.01$; ***$P < 0.001$. In all panels, the box, horizontal line, and whiskers represent interquartile range (IQR), median and 10%–90% percentile, respectively. Numbers in brackets on the *x*-axis indicate the number of livers analyzed for each group. The RP concentration in one NASH liver sample was below LOD. Hence the RP concentration in this liver was excluded from the data. The median concentrations and ranges of each retinoid in the three groups are listed in Table 3.

The Relative mRNA Expression of Retinoid-Related Genes in Normal and NAFLD Human Livers. The relative mRNA expression of several retinoid-related genes was measured in 48 normal liver samples (Fig. 5). This included analysis of genes responsible for hepatic retinol esterification (*LRAT*), for RA biosynthesis (*ALDH1A1*) and elimination (*CYP26A1*), and genes of nuclear receptors that RA and 4-oxo-RA isomers bind to and induce (*RARα* and *RARβ*). The relative mRNA expression of measured genes was variable in livers except for *LRAT*, for which the expression was fairly consistent. Surprisingly, none of the target gene mRNA expressions showed a significant correlation with the hepatic *at*RA concentration (Table 4), demonstrating that

mRNA expression should not be analyzed as a surrogate for retinoid concentrations. In the comparisons among the normal, steatosis, and NASH groups, the relative mRNA expression of *ALDH1A1* was significantly higher in the NASH livers than normal livers, whereas *RBP4* mRNA was significantly lower in the NAFLD livers compared with control (Supplemental Fig. S2). The relative mRNA expression of *LRAT*, *CYP26A1,* and *RARβ* was similar in the NAFLD and NASH groups compared with the normal (Supplemental Fig. S2).

Discussion

The goal of this study was to determine whether *at*RA concentrations in normal human livers and livers from donors with NAFLD correlate with commonly used markers of altered vitamin A homeostasis such as liver retinol and RP concentrations and retinoid-related mRNAs. Novel LC-MS/MS methods were developed for quantification of vitamin A metabolome in human liver. It is well known that different biologic matrices result in distinct interferences affecting analyte identification, recovery, matrix effects, and quantification. In addition, interferences from same tissue can vary with disease stages and between individuals. For example, NAFLD liver samples contain higher lipid content than normal liver samples, and liver tissue becomes fibrotic as the disease progresses. This may affect analyte recovery, ionization, and detection. Hence, accurate characterization of effects of NAFLD on hepatic vitamin A metabolome relies on good LC-MS/MS methods and appropriate internal standards to normalize extraction recovery and matrix effects. Validating bioanalytical methods is, however, particularly challenging for vitamin A metabolome as retinoids are endogenous molecules, and blank tissues do not exist for method development. It has been suggested that exposing tissues to light can be used to generate retinoid-depleted matrix such as serum (Arnold et al., 2012), but we did not observe a significant change in RA isomer concentrations in human liver samples after they were exposed to visible light for 1 hour (data not shown). This was probably the result of the low matrix transparency of the liver and high protein binding of retinoids. Therefore, to allow normalization for extraction recovery of the retinoids using isotope-labeled internal standards, LC-MS/MS methods for vitamin A metabolome were developed using retinoid-free charcoal-treated serum as a reference matrix and deuterated internal standards. The validity of this approach was confirmed by the determination that the slopes of the standard curves from liver and charcoal-treated serum were equal. Recovery of hepatic retinol and retinyl esters using the acetonitrile protein precipitation method developed here was confirmed by also measuring the concentrations of retinol and RP in 49 of 50 normal livers by the traditional hexane-extraction method (Obrochta et al., 2014; Grizotte-Lake et al., 2018) combined with isotope-labeled internal standards (Supplemental Fig. S3). No significant differences were observed between these methods.

Using the novel LC-MS/MS methods, human hepatic vitamin A metabolome was characterized for the first time in a relatively large sample of normal livers. The median concentrations of human hepatic retinol and RP reported in the current study are comparable with those measured previously by LC-UV methods in smaller samples (Schmitz et al., 1991; Schmidt et al., 2003). However, the analysis of human liver vitamin A metabolome discovered several species differences between human and mouse liver. The concentrations of *at*RA (14.0–579.5 pmol/g) and 13-*cis*RA (1.4–43.5 pmol/g) in human livers were 3- to 100-fold higher than those reported in mouse livers, in which *at*RA concentrations are about 5–20 pmol/g and 13-*cis*RA is below the limit of detection (Obrochta et al., 2014; Grizotte-Lake et al., 2018). This difference may have biologic significance, as laboratory mice may be more prone to RA deficiency than humans owing to the lower baseline RA concentrations. In addition, 4-oxo-*at*RA, an active retinoid that binds to retinoic acid receptors, was for the first time detected in the liver. This is a significant finding as 4-oxo-*at*RA has been shown to be more potent retinoid than *at*RA in anteroposterior axis formation and bind to RARs with affinity similar to *at*RA (Pijnappel et al., 1993; Idres et al., 2002; Topletz et al., 2015). In the human liver the concentrations of 4-oxo-*at*RA were comparable to that of *at*RA and 13-*cis*RA. However, the concentrations of 4-oxo-*at*RA were below the limit of quantitation in mouse livers and 4-oxo-13-*cis*RA was undetectable (Fig. 4). The lack of detection of 4-oxo-RA isomers in the liver previously is probably a result of this lack of 4-oxo-RA in mouse liver and the poor extraction recovery of 4-oxo-RA isomers by the common hexane extraction used for RA isomers in various tissues. The differences in RA and 4-oxo-*at*RA concentrations between human and mouse livers are surprising, as the retinyl esters and retinol concentrations in human livers (retinol 14.1 mol/g, RP 276 nmol/g) were similar to what have been reported in mouse livers (9.6 nmol/g retinol and 560 nmol/g retinyl esters) (Kane et al., 2008). However, the variability in retinyl ester concentrations in human livers was much greater than that in mouse livers. Further studies are needed to address the apparent species differences, the biochemical processes that drive these differences, and the consequences in retinoid signaling in various disease models.

Serum retinol and RBP4 concentrations, and liver retinol and retinyl ester concentrations, together with mRNA expression of retinoid-related genes are often used as indirect measures of altered *at*RA concentrations and signaling, as dietary vitamin A deficiency has been shown to lead to decreased concentrations of these retinoids and decreased retinoid signaling (Tanumihardjo, 2012). We aimed to test whether, in a sufficiently large set of human livers, these findings of correlations between retinoid concentrations in vitamin A deficiency could be extrapolated to retinoid homeostasis in other biologic scenarios. Our analysis shows a clear correlation between all retinoids in normal human livers (Table 4). However, the correlation between *at*RA concentrations and retinol disappeared when livers from subjects with NAFLD were included in the analysis, demonstrating that retinol concentrations cannot be used as a surrogate measure of liver *at*RA status. Surprisingly, no significant correlations were observed between any retinoid-related mRNAs and *at*RA concentrations (Table 4). Previous in vitro and animal studies have established that the mRNA expression of *LRAT*, *CYP26A1*, *RARα*, and *RARβ* can be induced in response to increased *at*RA concentrations (Napoli, 2012; Di Masi et al., 2015), and therefore we expected the mRNAs of these genes to correlate with *at*RA concentrations. However, our data unequivocally shows a lack of correlation between the mRNAs and *at*RA concentrations, demonstrating that measuring retinoid-related gene

expression is insufficient to reveal potential alterations in vitamin A metabolome. The data also suggest that *at*RA-induced changes in mRNA expression of these genes may only be captured within a specific time-window after an intervention. Of note, in the NAFLD samples, *ALDH1A1* mRNA was significantly increased, whereas *at*RA concentrations were decreased, potentially owing to feedback regulation of *ALDH1A1* mRNA in the liver. This finding is also in agreement with the weak negative correlation between *at*RA concentrations and *ALDH1A1* mRNA in normal livers although causality of these observations cannot be defined.

Circulating concentrations of retinoids have also been used as markers of altered retinoid signaling in disease states. However, the data collected here from human liver suggest that serum retinoids do not reflect tissue retinoid profiles. The median liver concentrations of *at*RA and 13-*cis*RA were 2- to 10-fold higher than what has been reported in human systemic circulation (Arnold et al., 2012). In addition, although the median concentration of 13-*cis*RA in human serum is higher than *at*RA, the liver *at*RA concentrations were about 5-fold higher than those of 13-*cis*RA. While these findings are not from matched donors and hence may be confounded, they strongly suggest that if circulating retinoid profiles are used in clinical studies as biomarkers of retinoid homeostasis, more research is needed to establish the biochemical processes that regulate the distribution of retinoids between tissues and systemic circulation. It is possible that interconversion kinetics between isomers in various tissues affect RA isomer distribution. Likewise, differences in the binding affinity to cellular (and plasma)-binding proteins may drive differences in tissue-to-serum concentration ratios. Previous studies have shown that *at*RA exhibits much higher binding affinity to cellular retinoic acid binding proteins ($K_d < 20$ nM) than does 13-*cis*RA ($K_d > 150$ nM) (Fiorella and Napoli, 1991; Fiorella et al., 1993). These differences may drive higher tissue partitioning of *at*RA compared with 13-*cis*RA and cause higher cellular unbound fractions of 13-*cis*RA than do the all-*trans* isomers.

The findings shown here of depleted vitamin A stores and *at*RA concentrations in NAFLD are in agreement with previous findings in mouse models. Progression to vitamin A deficiency in NAFLD is believed to be associated with hepatic stellate cell differentiation and reduced retinyl ester storage (Shirakami et al., 2012; Saeed et al., 2017). The current study strongly supports the model that during disease progression in NAFLD, hepatic retinyl ester, *at*RA, 13-*cis*RA, and 4-oxo-*at*RA concentrations are progressively diminished. However, unexpectedly, despite the significant depletion of retinyl esters and *at*RA, hepatic retinol concentrations were unchanged regardless of the disease progression. It is important to note that these observations were not collected as a prospective study, and prospective studies designed and powered on the basis of these observations are needed to further establish the progression and the extent of depletion of vitamin A storage in NAFLD.

In conclusion, the human hepatic vitamin A metabolome was quantified using novel LC-MS/MS methods and deuterated internal standards, providing a foundational understanding of the retinoid homeostasis in normal human liver. Additionally, the alterations of hepatic vitamin A metabolome were also defined in NAFLD liver samples to reveal the disease effects on vitamin A deficiency. These

data show that vitamin A metabolome is profoundly altered in NAFLD, and that the complete vitamin A metabolome should be analyzed to characterize disease effects on retinoid signaling and concentrations.

References

Amengual J, Ribot J, Bonet ML, and Palou A (2010) Retinoic acid treatment enhances lipid oxidation and inhibits lipid biosynthesis capacities in the liver of mice. *Cell Physiol Biochem* **25**:657–666.

Arnold SL, Kent T, Hogarth CA, Schlatt S, Prasad B, Haenisch M, Walsh T, Muller CH, Griswold MD, Amory JK, et al. (2015) Importance of ALDH1A enzymes in determining human testicular retinoic acid concentrations. *J Lipid Res* **56**: 342–357.

Arnold SLM, Amory JK, Walsh TJ, and Isoherranen N (2012) A sensitive and specific method for measurement of multiple retinoids in human serum with UHPLC-MS/MS. *J Lipid Res* **53**:587–598.

Botella-Carretero JI, Balsa JA, Vázquez C, Peromingo R, Díaz-Enriquez M, and Escobar-Morreale HF (2010) Retinol and alpha-tocopherol in morbid obesity and nonalcoholic fatty liver disease. *Obes Surg* **20**:69–76.

Chaves GV, Pereira SE, Saboya CJ, Spitz D, Rodrigues CS, and Ramalho A (2014) Association between liver vitamin A reserves and severity of nonalcoholic fatty liver disease in the class III obese following bariatric surgery. *Obes Surg* **24**: 219–224.

di Masi A, Leboffe L, De Marinis E, Pagano F, Cicconi L, Rochette-Egly C, Lo-Coco F, Ascenzi P, and Nervi C (2015) Retinoic acid receptors: from molecular mechanisms to cancer therapy. *Mol Aspects Med* **41**:1–115.

FDA (2018) *Bioanalytical Method Validation Guidance for Industry*. Center for Drug Evaluation and Research, Silver Spring, MD.

Fiorella PD, Giguère V, and Napoli JL (1993) Expression of cellular retinoic acid-binding protein (type II) in Escherichia coli. Characterization and comparison to cellular retinoic acid-binding protein (type I). *J Biol Chem* **268**:21545–21552.

Fiorella PD and Napoli JL (1991) Expression of cellular retinoic acid binding protein (CRABP) in Escherichia coli. Characterization and evidence that holo-CRABP is a substrate in retinoic acid metabolism. *J Biol Chem* **266**:16572–16579.

Graham TE, Yang Q, Blüher M, Hammarstedt A, Ciaraldi TP, Henry RR, Wason CJ, Oberbach A, Jansson P-A, Smith U, et al. (2006) Retinol-binding protein 4 and insulin resistance in lean, obese, and diabetic subjects. *N Engl J Med* **354**: 2552–2563.

Grizotte-Lake M, Zhong G, Duncan K, Kirkwood J, Iyer N, Smolenski I, Isoherranen N, and Vaishnava S (2018) Commensals suppress intestinal epithelial cell retinoic acid synthesis to regulate interleukin-22 activity and prevent microbial dysbiosis. *Immunity* **49**:1103–1115.e6.

Gundersen TE and Blomhoff R (2001) Qualitative and quantitative liquid chromatographic determination of natural retinoids in biological samples. *J Chromatogr A* **935**:13–43.

Idres N, Marill J, Flexor MA, and Chabot GG (2002) Activation of retinoic acid receptor-dependent transcription by all-trans-retinoic acid metabolites and isomers. *J Biol Chem* **277**:31491–31498.

Kane MA, Folias AE, Wang C, and Napoli JL (2008) Quantitative profiling of endogenous retinoic acid in vivo and in vitro by tandem mass spectrometry. *Anal Chem* **80**:1702–1708.

Kane MA and Napoli JL (2010) Quantification of endogenous retinoids. *Methods Mol Biol* **652**:1–54.

Kang HW, Bhimidi GR, Odom DP, Brun PJ, Fernandez ML, and McGrane MM (2007) Altered lipid catabolism in the vitamin A deficient liver. *Mol Cell Endocrinol* **271**: 18–27.

Kedishvili NY (2016) Retinoic acid synthesis and degradation. *Subcell Biochem* **81**: 127–161.

Kim SC, Kim CK, Axe D, Cook A, Lee M, Li T, Smallwood N, Chiang JYL, Hardwick JP, Moore DD, et al. (2014) All-trans-retinoic acid ameliorates hepatic steatosis in mice by a novel transcriptional cascade. *Hepatology* **59**:1750–1760.

Liu Y, Chen H, Wang J, Zhou W, Sun R, and Xia M (2015) Association of serum retinoic acid with hepatic steatosis and liver injury in nonalcoholic fatty liver disease. *Am J Clin Nutr* **102**:130–137.

Livak KJ and Schmittgen TD (2001) Analysis of relative gene expression data using real-time quantitative PCR and the 2(-delta delta C(T)) method. *Methods* **25**: 402–408.

Napoli JL (2012) Physiological insights into all-trans-retinoic acid biosynthesis. *Biochim Biophys Acta* **1821**:152–167.

Obrochta KM, Kane MA, and Napoli JL (2014) Effects of diet and strain on mouse serum and tissue retinoid concentrations. *PLoS One* **9**:e99435.

O'Byrne SM and Blaner WS (2013) Retinol and retinyl esters: biochemistry and physiology. *J Lipid Res* **54**:1731–1743.

Pijnappel WW, Hendriks HF, Folkers GE, van den Brink CE, Dekker EJ, Edelenbosch C, van der Saag PT, and Durston AJ (1993) The retinoid ligand

4-oxo-retinoic acid is a highly active modulator of positional specification. *Nature* **366**:340–344.

Saeed A, Dullaart RPF, Schreuder TCMA, Blokzijl H, and Faber KN (2017) Disturbed vitamin A metabolism in non-alcoholic fatty liver disease (NAFLD). *Nutrients* **10**.

Schmidt CK, Brouwer A, and Nau H (2003) Chromatographic analysis of endogenous retinoids in tissues and serum. *Anal Biochem* **315**:36–48.

Schmitz HH, Poor CL, Wellman RB, and Erdman JW Jr (1991) Concentrations of selected carotenoids and vitamin A in human liver, kidney and lung tissue. *J Nutr* **121**:1613–1621.

Shiota G (2005) Loss of function of retinoic acid in liver leads to steatohepatitis and liver tumor: a NASH animal model. *Hepatol Res* **33**:155–160.

Shirakami Y, Lee SA, Clugston RD, and Blaner WS (2012) Hepatic metabolism of retinoids and disease associations. *Biochim Biophys Acta* **1821**:124–136.

Stevison F, Hogarth C, Tripathy S, Kent T, and Isoherranen N (2017) Inhibition of the all-trans retinoic acid (atRA) hydroxylases CYP26A1 and CYP26B1 results in dynamic, tissue-specific changes in endogenous atRA signaling. *Drug Metab Dispos* **45**:846–854.

Suano de Souza FI, Silverio Amancio OM, Saccardo Sarni RO, Sacchi Pitta T, Fernandes AP, Affonso Fonseca FL, Hix S, and Ramalho RA (2008) Non-alcoholic fatty liver disease in overweight children and its relationship with retinol serum levels. *Int J Vitam Nutr Res* **78**:27–32.

Tanumihardjo SA (2012) Biomarkers of vitamin A status: what do they mean?, in *WHO Report: Priorities in the Assessment of Vitamin A and Iron Status in Populations*, World Health Organization, Panama City, Panama.

Topletz AR, Tripathy S, Foti RS, Shimshoni JA, Nelson WL, and Isoherranen N (2015) Induction of CYP26A1 by metabolites of retinoic acid: evidence that CYP26A1 is an important enzyme in the elimination of active retinoids. *Mol Pharmacol* **87**:430–441.

Trasino SE, Tang XH, Jessurun J, and Gudas LJ (2015) Obesity leads to tissue, but not serum vitamin A deficiency. *Sci Rep* **5**:15893.

Villaça Chaves G, Pereira SE, Saboya CJ, and Ramalho A (2008) Non-alcoholic fatty liver disease and its relationship with the nutritional status of vitamin A in individuals with class III obesity. *Obes Surg* **18**:378–385.

Ziouzenkova O, Orasanu G, Sharlach M, Akiyama TE, Berger JP, Viereck J, Hamilton JA, Tang G, Dolnikowski GG, Vogel S, et al. (2007) Retinaldehyde represses adipogenesis and diet-induced obesity. *Nat Med* **13**:695–702.

Address correspondence to: Dr. Nina Isoherranen, Department of Pharmaceutics, School of Pharmacy, University of Washington, Health Science Building, Room H-272M, Box 357610, Seattle, WA 98195-7610. E-mail: ni2@uw.edu

Supplemental data for:

Characterization of Vitamin A Metabolome in Human Livers with and without NAFLD

Guo Zhong, Jay Kirkwood, Kyoung-Jae Won, Natalie Tjota, Hyun-Young Jeong, Nina

Isoherranen

Department of Pharmaceutics, University of Washington, Seattle, WA (G.Z., J.K., N.T., N.I.);

Department of Pharmacy Practice, University of Illinois, Chicago, IL (K.W., H.J.)

Table S1. Donor information of the 50 normal livers from Corning. Detailed donor information including medication histories can be requested from Corning www.corning.com/lifesciences. AA, African American; A, Asian; C, Caucasian; M, male; F, female; CMV, cytomegalovirus; CVA, cerebrovascular accident; ICH, intracerebral hemorrhage; GSW, gunshot wound.

Lot	Age (yrs)	Ethnicity	Gender	Cause of Death	Smoker	CMV Serology
HH207	59	C	M	Cerebrovascular/Stroke	Yes	positive
HMAA213	68	AA	M	CVA	Yes	positive
HMA357	55	A	M	Anoxia - Cardiovascular	No	positive
HFA390	75	A	F	ICH - Stroke	No	positive
HH501	36	C	F	GSW to the head	No	positive
HH503	22	C	M	Closed head injury	Yes	positive
HH506	21	C	M	Gunshot wound to the head	Yes	positive
HH509	44	C	M	Closed head injury/ motorcycle vs car	Yes	positive
HH521	25	C	M	Self-inflicted GSW	No	negative
HH523	52	C	M	Anoxic Injury	Yes	positive
HH528	51	C	M	Intracranial bleed	Yes	positive
HH533	36	C	M	Traumatic brain injury, s/p hit head on steps	Yes	negative
HH534	32	C	M	ICH	Yes	negative
HH535	64	C	F	Subarachnoid hemorrhage	Yes	negative
HH539	38	C	M	Severe closed head injury and bleed	No	negative

HH549	47	C	M	Subarachnoid hemorrhage	No	positive
HH552	47	C	M	Brainstem stroke	Yes	positive
HH553	68	C	F	subdural hematoma, ICH, subarachnoid hemorrhage s/p fall	Yes	positive
HH557	36	C	M	ICH s/p motorcycle accident	Yes	negative
HH560	58	C	F	GSW to the head	No	negative
HH564	40	C	M	Subarachnoid hemorrhage s/p aneurysm	Yes	positive
HH566	40	C	M	Anoxia	Yes	positive
HH574	32	C	M	Cardiac arrest	Yes	positive
HH575	66	C	M	Cardiac arrest	Yes	positive
HH576	48	C	M	Intracranial bleed	No	positive
HH577	53	C	M	Stroke	Yes	negative
HH582	38	C	M	ICH	Yes	negative
HH585	59	C	M	Cardio vascular accident	Yes	positive
HH613	33	C	F	Anoxia s/p seizure	No	positive
HH623	62	C	M	CVA, ICH	Yes	negative
HH641	53	C	M	CVA	Yes	negative
HH652	68	C	M	CVA	Yes	negative
HH661	24	C	M	Head trauma s/p motor cycle accident	Yes	negative
HH677	63	C	F	Subarachnoid hemorrhage	Yes	positive
HH680	66	A	M	Head trauma s/p motor vehicle accident	Yes	positive

HH704	41	C	M	Head trauma s/p motor cycle accident	No	positive
HH705	42	H	F	Intracranial hemorrhage	No	positive
HH715	46	C	M	Anoxia	No	negative
HH724	49	C	M	Cardio vascular accident s/p sortic dissection	No	negative
HH741	68	C	M	Head trauma s/p head struck on concrete	No	negative
HH746	65	C	M	Head injury s/p tractor accident	Yes	positive
HH755	42	C	F	subdural hematoma, CVA s/p aneurysm	Yes	positive
HH790	55	C	F	CVA, ICH	No	positive
HH795	44	C	M	Anoxia, asphyxation	No	negative
HH804	49	C	F	Anoxia, CVA	Yes	positive
HH840	80	A	M	CVA, ICH	No	positive
HH848	53	C	M	CVA	Yes	positive
HH860	63	AA	F	CVA, ICH	Yes	positive
HH867	26	AA	M	Head trauma, GSW	Yes	negative
HH868	66	A	M	CVA, ICH	No	negative

.

Table S2. Donor information of NAFLD liver samples obtained from Liver Tissue Cell Distribution System (https://www.pathology.umn.edu/research/liver-tissue-cell-distribution-system). F, female; M, male; ESLD, end-stage liver disease.

	sample ID	Gender	Age	Ethnicity	Diagnosis	Cause of death	Obesity or Diabetes
Steatosis n=9	642	F	32	N/A	90% steatosis	Anoxia	N/A
	747	F	55	N/A	100 % steatosis	Intracerebral hemorrhage	N/A
	814	F	33	N/A	90 % steatosis	Bacterial meningitis	N/A
	982	F	50	N/A	75 % steatosis	Cerebrovascular accident	N/A
	1020	M	45	N/A	80% steatosis	Hypertension	N/A
	1038	M	47	N/A	80% steatosis	Subarachnoid hemorrhage	N/A
	1124	M	40	N/A	80% steatosis	Intracerebral hemorrhage	N/A
	1068	F	50	N/A	75% steatosis	Subdural hematoma	N/A
	1233	M	32	N/A	75% steatosis	Hypertension	N/A
NASH n=13	1228	M	62	N/A	ESLD secondary to NASH	N/A	Type II diabetes
	1242	F	43	White	ESLD secondary to NASH	N/A	
	1247	F	52	Hispanic	ESLD secondary to NASH	N/A	
	1249	F	55	White	NASH, Cirrhosis	N/A	Obesity
	1259	M	56	White	NASH, Cirrhosis	N/A	
	1305	F	48	White	NASH, Cirrhosis	N/A	Obesity

| 1338 | M | 64 | White | Cirrhosis clinically secondary to NASH | N/A | Obesity |
1370	M	53	White	NASH, Cirrhosis	N/A	Type II diabetes
1443	M	68	White	ESLD secondary to NFALD, Cirrhosis	N/A	Type II diabetes
1552	F	43	White	ESLD secondary to NASH	N/A	Obesity
1569	M	42	White	NASH Cirrhosis	N/A	Type II diabetes, obesity
1509	M	68	N/A	Cirrhosis with chronic hepatitis, medical history of steatosis	N/A	Type II diabetes
1533	M	70	White	Cirrhosis with mild active chronic hepatitis, medical history of steatosis	N/A	Type II diabetes, obesity
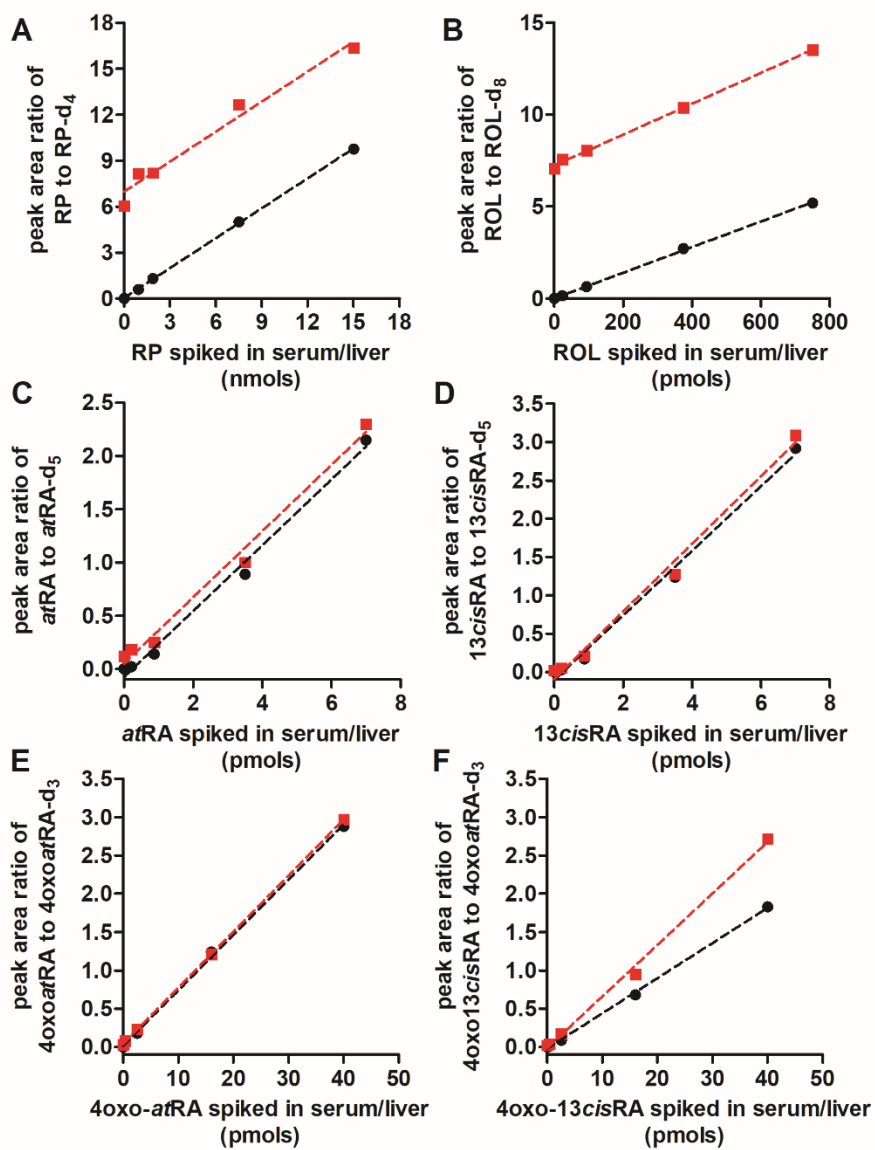
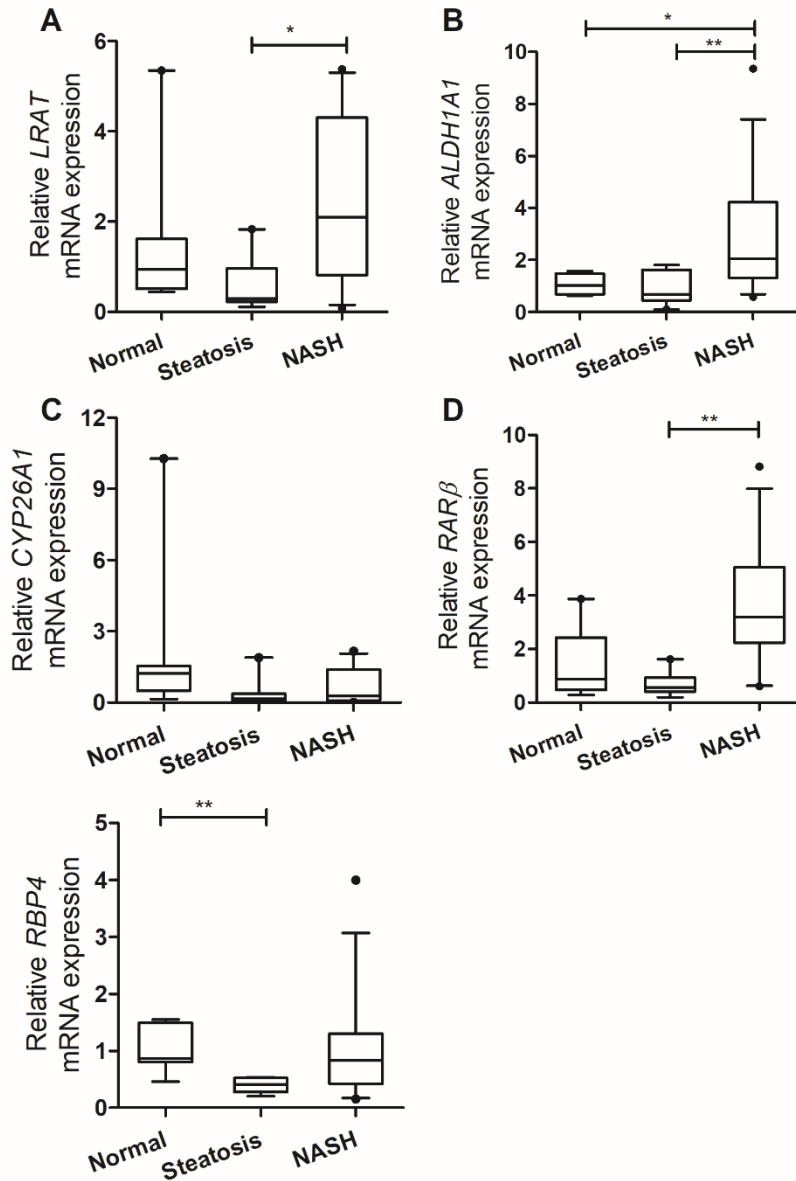Figure S1. Retinoid standard curves constructed in serum (black) and mouse liver homogenates (red).

Figure S2. Relative mRNA expression of retinoid target genes in normal and NAFLD human livers. The relative mRNA expression of *LRAT* (A), *ALDH1A1* (B), *CYP26A1* (C), *RARβ* (D) and *RBP4* (E) were calculated using $2^{(-\Delta\Delta Ct)}$ method with *GAPDH* as the house-keeping gene; $\Delta\Delta Ct = \Delta C_t - Avg\Delta C_{t, normal}$. Sample numbers are 9, 9 and 13 in the normal, steatosis and NASH groups, respectively. The box, horizontal bar and whiskers represent interquartile range (IQR), median and 10-90% percentile, respectively. All the data were analyzed with Kruskal-Wallis test followed by Dunn's multiple comparison; *, $P < 0.05$; **, $P < 0.01$.
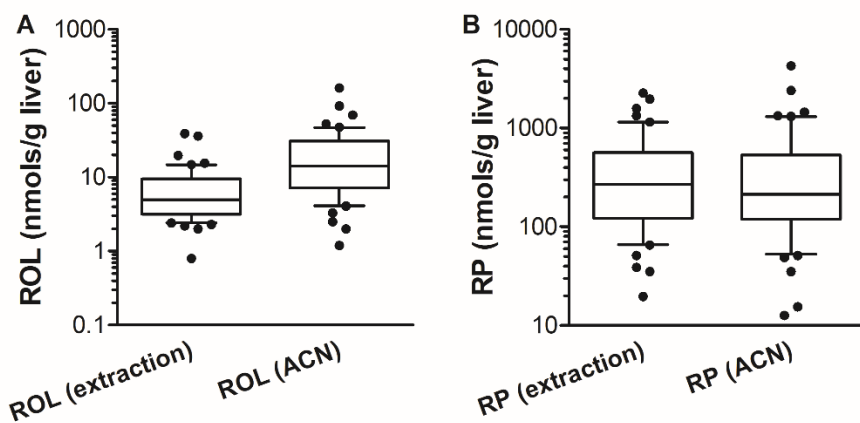
Figure S3. Hepatic concentrations of ROL and RP in normal human liver samples measured by hexane extraction method (n=49) and acetonitrile (ACN)-precipitation method (n=50).